

# A Real Space Glue for Cuprate Superconductors

Xiuqing Huang<sup>1,2\*</sup>

<sup>1</sup>Department of Physics and National Laboratory of Solid State Microstructure, Nanjing University, Nanjing 210093, China

<sup>2</sup>Department of Telecommunications Engineering ICE, PLAUST, Nanjing 210016, China

(Dated: August 6, 2017)

In a recent article [Science **317**, 1705 (2007)], Anderson pointed out that many theories about electron pairing in cuprate superconductors may be on the wrong track and there is no reason to believe that the dynamic screening ( $\mathbf{k}$ -space) can provide a valid “glue” to hold the electron pairs together. On the other hand, the most recent experimental observations imply the possible generic existence of the real space localized Cooper pairs in amorphous insulating and other nonsuperconducting systems [M. D. Stewart Jr. *et al.*, Science **318**, 1273 (2007)]. It is therefore clear that the “glue” for high- $T_c$  superconductors is relevant to the real space correlations. In this paper, we argue that real space electron-electron interactions can play the role of “glue” in high- $T_c$  superconductors. It is found that two localized electrons, due to a real space Coulomb confinement effect, can be in pairing inside a single plaquette of the CuO plane. The scenario suggests appearance of a dominating  $d$ -wave-like pairing symmetry in the hole-doped cuprates, while a more complex mixed ( $s + d$ ) symmetry in the electron-doped cuprates. Based on the mechanism, the relationships between the superconductivity and the charge-stripe order are discussed. In the  $\text{La}_{2-x}\text{Sr}_x\text{CuO}_4$  (LSCO) with  $1/18 \leq x \leq 1/4$ , we show that the paired electrons can self-organize into the dimerized Wigner crystal. Two kinds of quasi-one-dimensional metallic magnetic-charge stripes, where the superconductivity and dynamical spin density wave (SDW) coexist, are analytically determined. Furthermore, the physical original of the magic doping fractions (at  $x = 1/4, 1/8, 1/9, 1/16$  and  $1/18$ ) of superconductivity and an analytical phase diagram for LSCO are given.

PACS numbers: 74.20.-z, 74.20.Mn, 74.20.Rp, 74.25.Dw

## I. INTRODUCTION

It has been over two decades since the first discovery of high- $T_c$  superconductivity (HTSC) in copper oxide materials<sup>1</sup>. Theoretically, soon after the discovery of the high- $T_c$  cuprates, the resonating valence bond (RVB) theory, a strong coupling version of the spin fluctuation approach, was introduced by Anderson<sup>2</sup>. After Anderson’s original conjecture, Zhang and Rice derived a single-band effective Hamiltonian for HTSC cuprates<sup>3</sup>. Wen and Lee developed the SU(2)-gauge theory of the strong coupling nature for the doped  $t$ - $J$  model<sup>4</sup>. Varma and co-workers established the marginal Fermi liquid theory to explain many of the anomalous behaviors in cuprates<sup>5</sup>. Zhang proposed a very interesting and unified theory based on the SO(5) symmetry of superconducting (SC) and antiferromagnetic (AF) phases<sup>6</sup>. Moreover, Dagotto<sup>7</sup> and Lee *et al.*<sup>8</sup> gave comprehensive reviews of the mechanisms of the HTSC. In spite of extensive theoretical efforts, the mechanism of the HTSC in the cuprates remains a profound unsolved mystery of modern physics. Now, the majority view on the mechanism is that the weak-coupling mean-field BCS theory<sup>9</sup>, which is based on electron-phonon interaction, may not be suitable for the high superconducting transition caused by strong correlations. Experimentally, accumulating evidences show that the pairing mechanism of HTSC is relevant to the real-space (a localized picture) electron-electron correlations. One of the most striking experimental fact is the observation of a periodic pattern in the local electron density of states (LDOS) by high resolution scanning tunneling microscopy (STM)<sup>10</sup>. Furthermore, one of the most ex-

citing experimental evidences in favor of the localized Cooper pairs have just been reported<sup>11</sup>, the excellent experiment implies the possible generic existence of the real space superconducting pair correlations in amorphous insulating and other nonsuperconducting systems such as underdoped high- $T_c$  superconductors above  $T_c$ .

Very recently, Anderson pointed out that many theories about electron pairing in cuprate superconductors may be on the wrong track<sup>12</sup>. In the paper, it is clearly shown that the framework of dynamic screening (quasi-particle) is impossible to provide the “glue” for the high- $T_c$  copper oxide superconductors, as the net interaction between electrons is always repulsive. If this is the correct viewpoint, but what will be the “glue” binding the electrons in pairs?

Compared to conventional superconductors, besides their exceptionally high superconducting transition temperatures, there are many anomalous physical properties in high- $T_c$  cuprates. It appears to be generally accepted that conventional BCS superconductors are characterized by a standard  $s$ -wave, while the symmetry of the high- $T_c$  superconducting order parameter is believed to be  $d$ -wave for the hole-doped ( $p$ -type) cuprates<sup>13,14,15</sup>. However, for the electron-doped ( $n$ -type) cuprates there is much controversy about whether the order parameter has a  $s$ -wave symmetry<sup>16,17</sup>, or  $d$ -wave<sup>18,19,20,21</sup>, or a nonmonotonic  $d$ -wave<sup>22</sup>, or a crossover from a  $d$ -wave symmetry for underdoped compositions to a  $s$ -wave symmetry for the overdoped region<sup>23,24</sup>. Moreover, it has been one of the experimental facts that underdoped cuprates possess a pseudogap<sup>25,26</sup> in the non-superconducting state with anomalous physical properties below a temperature

$T^* > T_c$ . The origin of the pseudogap has become a challenging issue as it might eventually lead to identify the superconducting mechanism. A class of theoretical models attempted to describe the pseudogap state as a precursor of the superconducting  $d$ -wave gap<sup>27</sup>.

To date, more experimental results indicate that the charge-ordered stripes in cuprates represent a specific type of order that has been experimentally observed to compete with superconductivity<sup>28,29,30,31</sup>. The stripes are a real-space pattern, in which the charge carriers condense into rivers of charge separated by insulating domains<sup>28</sup>. Generally, stripes are classified as metallic or insulating. It is considered that the static stripe order (insulating) is bad for superconductivity and is responsible for the suppression of the superconducting transition temperature<sup>31</sup>, while the dynamic stripes (metallic) are essential to the superconductivity in the cuprates<sup>27,32,33</sup>. More recently, strong experimental evidence from the STM studies suggest the presence of a 4-lattice constant checkerboard charge order in underdoped cuprates at the doping level 1/8, which are referred to as the “1/8 anomaly”<sup>10,34,35,36,37</sup>. In addition, the checkerboard-type ordering of the charge carriers at “magic doping fractions” have been intensively studied<sup>38,39,40,41</sup>. Castellani *et al.*<sup>42</sup> have suggested that such commensurate stripes should be insulating. Furthermore, the underlying crystalline electronic orders (or Wigner crystals) of charge carriers in cuprates of low doping level have been proposed<sup>38,39,43</sup>. In view of these interesting experimental results and heuristic theoretical proposals, it is now a clear viewpoint that any interpretation of superconductivity in the cuprates must account for the real-space charge stripes.

The goal of the present paper is to unveil the mystery of high- $T_c$  superconductivity. We argue that the mechanism of superconductivity in both electron-doped and hole-doped cuprate superconductors should be established on a picture of pure electrons. We show that this scenario can be used to explain the basic phenomenology of the high- $T_c$  superconductors from the pairing mechanism to charge stripes. We attempt to provide answers to the following open questions: Are the pairing and superconducting mechanism of the electron- and hole-doped cuprates different? What will be the “glue” to hold the electron pairs together? What is the one-dimensional nature of the stripes? Are they insulators or metals? Do the stripes compete with superconductivity, help superconductivity or hinder it?

## II. CHARGE CARRIERS: ELECTRONS OR HOLES?

Ever since the discovery of high-temperature superconductivity, many different cuprate superconductors were synthesized. It should be noted that though the structures of these materials may be different, the essential structure to be concerned about is that of the same two-

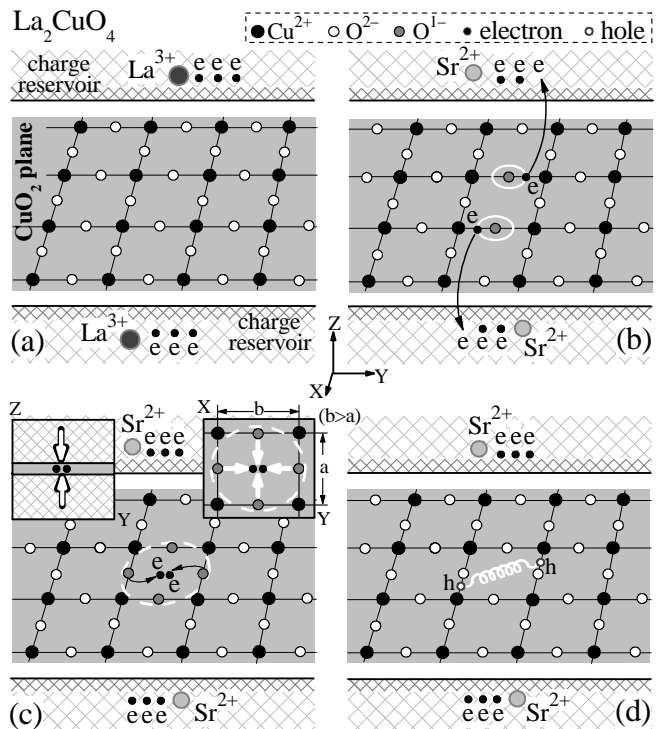


FIG. 1: The charge carriers and the Coulomb confinement of electrons in the CuO<sub>2</sub> plane of cuprate superconductor. (a) The insulating parent compound of La<sub>2-x</sub>Sr<sub>x</sub>CuO<sub>4</sub>, (b) the partially substitution of Sr<sup>2+</sup> for La<sup>3+</sup>, (c) two localized charge carriers of undressed electrons, insets indicate the Coulomb confinement on these electrons, and (d) the conventional dressed holes picture.

dimensional CuO<sub>2</sub> planes in them. In particular, the so-called hole-doped La<sub>2-x</sub>Sr<sub>x</sub>CuO<sub>4</sub>, due to its relatively simpler structure but a more complex phase diagram, is the best studied material. The La<sub>2</sub>CuO<sub>4</sub> [see Fig. 1(a)], the parent compound of La<sub>2-x</sub>Sr<sub>x</sub>CuO<sub>4</sub>, is an insulator. As shown in Fig. 1 (b), the partial substitution of Sr<sup>2+</sup> for La<sup>3+</sup> will result in a deficiency of electrons in the charge reservoirs and a leaving of electrons from O ions (O<sup>2-</sup>) of CuO<sub>2</sub> planes to the charge reservoirs. To maintain the local symmetry and the stability of the CuO<sub>2</sub> plane, the other two O<sup>2-</sup> (adjacent the O<sup>1-</sup>) tend to donate two electrons which would likely to be trapped in the center of the four O<sup>1-</sup> [Fig. 1(c)]. Physically, the effect of the local distortion pattern in Fig. 1(c) is to minimize the system’s energy. In this case, these two electrons will experience a strong real space Coulomb confinement [see insets of Fig. 1(c)] imposed by the charge reservoirs and the local structure distortion in the CuO<sub>2</sub> plane. It should be noted that the central character (charge carrier) in this paper is in fact not the artificial hole, but the real electron.

Normally, quantum theory assumes that the charge carriers prefer to stay and travel (or hopping) in the most “crowded” and complicated Cu–O chains, as shown in

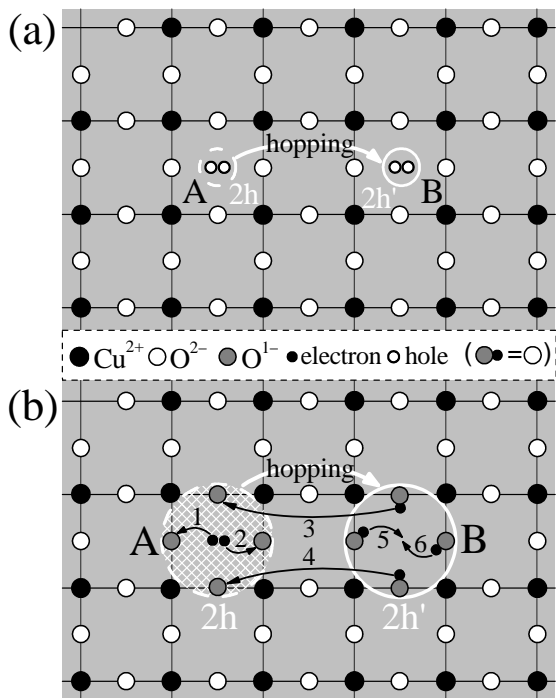


FIG. 2: A comparison between an idealized hole pair (sizeless quasiparticles) and a “real” hole pair. (a) The idealized hole pair can move (hopping from A to B) easily in  $\text{CuO}_2$  ( $\text{Cu}^{2+}$ ,  $\text{O}^{2-}$ ) plane. (b) The “real” hole pair can be considered as a dressed electron pair, the movement of one “real” hole pair (hopping from A to B) is truly equivalent to the much more complicated transfer of six electrons (indicated by 1, 2, 3, 4, 5 and 6).

Fig. 1(d). It now appears that the paired electrons (or holes) in the  $\text{CuO}_2$  planes has two possible choices, as shown in Fig. 1(c) and Fig. 1(d). Which situation would the pair be inclined to choose? If we believe that charge carriers do appear as suggested by quantum mechanics in the Cu–O chains [Fig. 1(d)], then there will be a strong Coulomb interaction among the charge carriers and the ions ( $\text{Cu}^{2+}$  and  $\text{O}^{2-}$ ), consequently increase the compound’s energy and this in turn could decrease the system’s stability. While for the case of Fig. 1(c), the Coulomb interaction among the charge carriers and the ions will be greatly reduced, as a result, increase the system’s stability. Therefore, we argue that the conventional hole-doping picture of Fig. 1(d) is physically inadequate.

Having applied the hole concept greatly in solid-state physics, we are faced with the challenge of constructing an effective physical picture for this mysterious quasiparticle: What would a hole pair look like if it did exist? The point of view taken here is that the “real” holes arise from unique chemical construction in  $\text{CuO}_2$  plan. It was assumed that, in the hole doped high- $T_c$  superconductors, the hole pairs (the sizeless particles carried a positive electric charge and a spin) can maintain their integrity in a square lattice and move [As shown in Fig.

2(a), hopping from A to B] easily and coherently in  $\text{CuO}_2$  ( $\text{Cu}^{2+}$ ,  $\text{O}^{2-}$ ) plane<sup>49</sup>. Here, it seems worthwhile to point out that this idealized picture of hole is physically untrue. As shown in Fig. 1(c), when the two electrons sit on the square lattice, we have a “real” hole pair as illustrated in Fig. 2(b). As one can see from the figure, it appears that the static hole pair (state A) can be thought of as a dressed electron pair in  $\text{CuO}_2$  ( $\text{Cu}^{2+}$ ,  $\text{O}^{2-}$ ) plane. However, it is shown that this “real” hole pair is structural unstable. A fatal difficulty occurs when the pair is moving from A to B [see Fig. 2(b)]. In this figure, it is clearly shown the simplest possible movement of one “real” hole pair, in fact, involving a very complicated transportation of six electrons (there are infinite possible ways to “move” the pair, note that only one set of possible movement of the electrons is indicated in the figure). Therefore, it is hard to imagine that the “real” hole pair can always maintain its integrity during the “hopping” process. On this basis, we argue that the artificial holes should be abandoned.

Anyway, one should be cautious when drawing conclusions based on the concept of “hole”. As emphasized by Hirsch, using the language of ‘holes’ rather than ‘electrons’ in fact obscures the essential physics since these electrons are the ones that ‘undress’ and carry the supercurrent (as electrons, not as holes) in the superconducting state<sup>50</sup>. In the following, we shall illustrate the superconductive properties of the so-called hole-doped high- $T_c$  cuprates in a pure electron picture (without the hole concept).

### III. PAIRING MECHANISM, PAIRING SYMMETRY AND PSEUDOGAP

In conventional superconductors, Bardeen, Cooper and Schrieffer (BCS)<sup>9</sup> argued that phonons (atomic lattice vibrations) act as the “glue” that binds the electron pairs together. But at high temperatures, the vibrational motion of the material’s lattice becomes so stiff that it tends to break up the electron pairs instead of holding them together<sup>12</sup>. So what could possibly provide the glue that keeps the carriers bound in Cooper pairs? Although many candidates for this glue (including spin fluctuations, phonons, polarons, charge stripes and spin stripes) have been proposed. However, what the pairing glue is in high- $T_c$  cuprates is still an open question. In this Section, I would like to discuss the issue from the point of view of real-space electron-electron interaction. To test this hypothesis, we are studying the pairing symmetry of electron- ( $n$ -type) and hole-doped ( $p$ -type) cuprate superconductors. The section ended with a brief discussion of pseudogap.

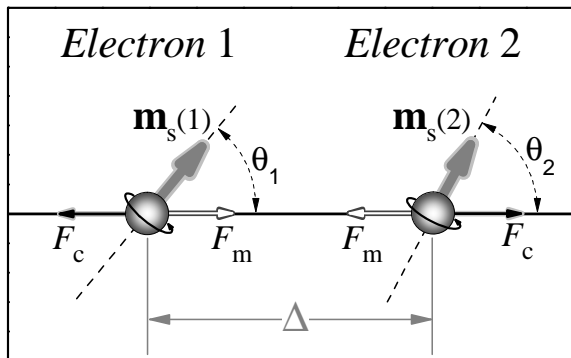


FIG. 3: The electromagnetic interaction between two electrons. Normally, there is a pair of long-range Coulomb repulsion  $F_c$ . In addition, two spinning electrons may create a pair of short-range attractive forces  $F_m$  due to the dipolar-dipolar interaction, which can act as the mysterious “glue” for electron pairs. If *electron 1* and *electron 2* are free, obviously, the long-range Coulomb repulsion  $F_c$  is dominant in comparison with the short-range attraction  $F_m$ , hence, the  $F_m$  can work as the “glue” only if the influence of the repulsion  $F_c$  between the electrons be successfully suppressed by the external confinement effects as shown in Fig. 1(c).

#### A. What is the “glue” for cuprate superconductors?

Since the observation of real-space ordering of charge in cuprate superconductors<sup>28,29,30,31</sup>, it is widely accepted that short-range electron-electron correlations can bind electrons into real space pairs and dominate the superconductivity properties of the materials. Normally, as shown in Fig. 3, for the two static electrons, there is a on-site long-range repulsive electron-electron Coulomb interaction

$$F_c = \frac{e^2}{4\pi\epsilon_0\Delta^2}, \quad (1)$$

where  $e$  is the electron charge and  $\Delta$  is the distance between two electrons. Due to this strong repulsion of Eq. (1) between electrons, the confinement scenario of Fig. 1(c) doesn’t mean that the targeted electrons can be naturally paired. So how can repulsive Coulomb forces exerted on electrons be eliminated so that the electrons can be in pairs?

It is known that study of superconducting correlations in conventional superconductors is always performed in momentum-space (dynamic screening), where the paired electrons are seldom or never in the same place at the same time<sup>12</sup>. In the case of dynamic screening, only the long-range Coulomb interaction  $e^2/\Delta$  is considered while the short-range electron–electron magnetic interactions is completely ignored. We argue here that, in the case of real-space screening, the magnetic forces among the electrons (see also Fig.3) could provide a strong “glue” for electron pairing leading to high- $T_c$  superconductivity in

cuprate superconductors. Approximately, the magnetic dipolar interaction forces  $F_m$  exerted on the electrons are given by

$$F_m \approx \frac{3\mu_0\mu_B^2}{2\pi\Delta^4} \cos\theta_1 \cos\theta_2, \quad (2)$$

where  $\mu_0$  is the permeability of free space and  $\mu_B$  is the Bohr magneton. The forces  $F_m$  can be attractive and repulsive depending on the orientation ( $\theta_1$  and  $\theta_2$ ) of electron magnetic moment  $\mathbf{m}_s(j)$ , ( $j = 1, 2$ ). When  $\theta_1 = \theta_2 = 0$  (or  $\pi$ ), the magnetic poles of the paired electrons are lined up in parallel, consequently, the attractive magnetic force reaches its maximum value  $F_m^{\max} = 3\mu_0\mu_B^2/2\pi\Delta^4$ . When  $F_c = F_m^{\max}$ , we have a stable electron pair with the distance  $\Delta_0$  as

$$\Delta_0 = \frac{\sqrt{6}\mu_B}{ec} \approx 4.73 \times 10^{-3} \text{ \AA}, \quad (3)$$

where  $c$  is the speed of light in vacuum.

Because of the short-range interaction characteristics of Eq. (2), as is usually the case  $F_c \gg F_m^{\max}$ , then it is clear that the “glue” (attractive magnetic force  $F_m^{\max}$ ) works only if the cuprate superconductors has the effect of weakening the long-range repulsive force  $F_c$ . We presume that the real-space confinement effect (electromagnetic interactions) in  $\text{CuO}_2$  plane [see Fig. 1(c)] plays a central role in suppressing the influence of the Coulomb repulsion between electrons. To describe this, two spin parallel electrons of Fig. 3 with a joint paired-electron magnetic moment  $\mathbf{M}_s = \mathbf{m}_s(1) + \mathbf{m}_s(2)$  are embedded into a  $\text{CuO}$  plane of the cuprate superconductor, as shown in Fig. 4. Looking at the figure, just a simplification, only nearest-neighbor and next-nearest-neighbor interactions are considered. Inside the unit cell, the possible paired-electrons with the magnetic moment  $\mathbf{M}_s$  along the  $\theta$  direction, and the corresponding distance between the electrons is reexpressed as  $\Delta(\theta)$ . From the figure, one can easily conclude that the pair with the  $\mathbf{M}_s$  oriented in (100), (010), ( $\bar{1}00$ ) and ( $0\bar{1}0$ ) directions is generally considered to be much more stable due to the suppression ( $F_1$ ) of the four oxygen ions ( $\text{O}^{1-}$  for hole-doped,  $\text{O}^{2-}$  for electron-doped), as opposed to the cases, in (110), ( $\bar{1}\bar{1}0$ ), ( $\bar{1}\bar{1}0$ ) and ( $1\bar{1}0$ ) directions where the bound pair tends to be separated by Coulomb forces ( $F_2$ ) of the  $\text{Cu}^{2+}$ . As a consequence, the distance  $\Delta(\theta)$  between the two electrons of the pair has a minimum at  $\theta = 0, \pi/2, \pi$  and  $3\pi/2$ , while at  $\theta = \pi/4, 3\pi/4, 5\pi/4$  and  $7\pi/4$ ,  $\Delta(\theta)$  will reach its maximum value. According to Eq. (2), the orientation dependence of binding energy for the electron pair within a single plaquette can be defined as

$$E_b(\theta) = \frac{\mu_0\mu_B^2}{2\pi\Delta^3(\theta)} \approx \frac{1.074 \times 10^{-3}}{\Delta^3(\theta)} (\text{eV}), \quad (4)$$

where the unit of distance  $\Delta(\theta)$  is angstrom.

It is important to note that no quasiparticles are involved in the above studies, hence the presented real

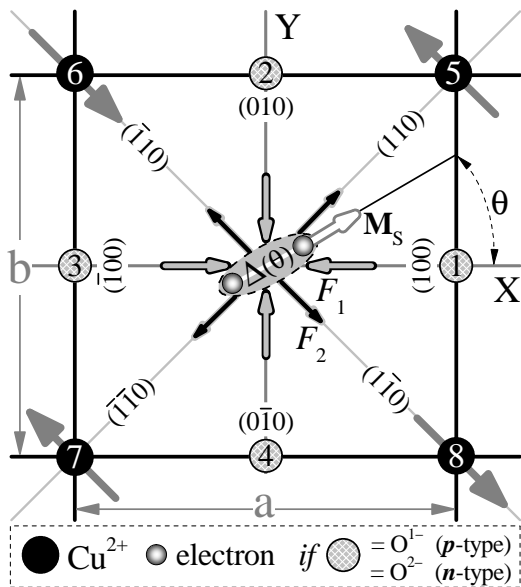


FIG. 4: Two spin parallel electrons with a joint magnetic moment  $\mathbf{M}_s$  is confined inside one unit cell of CuO plane. Only nearest-neighbor (1, 2, 3, 4) and next-nearest-neighbor (5, 6, 7, 8) interactions are considered. If  $\Delta(\theta) \ll a$ , approximately, there are four confinement forces ( $F_1$ ) in both the  $x$  and  $y$  directions, while four dissociated forces ( $F_2$ ) in the diagonal directions.

space pairing mechanism (“glue”) can be regarded as a self-pairing mechanism due to the intrinsic electromagnetic exchange coupling between the real electrons. There is no reason to believe that the dynamic screening (quasiparticle approximation) is related to a “glue” in the high- $T_c$  cuprates where the net interaction contributed by “quasiparticle” is found always repulsive, as emphasized by Anderson<sup>12</sup>.

### B. Pairing symmetry in $n$ -type and $p$ -type cuprate superconductors.

Now we turn to the pairing symmetry. In recent years a number of experiments have indicated that the predominant real-space  $d$ -wave symmetry in hole-doped cuprate superconductors<sup>51</sup>. Theoretical and numerical studies of the two-dimensional Hubbard  $t$ - $J$  models have also suggested  $d$ -wave pairing symmetry<sup>52</sup>. Altman and Auerbach have provided an intuitive picture of how  $d$ -wave hole pair can survive in a single plaquette<sup>49</sup>. On the other hand, pairing symmetry in electron-doped cuprate superconductors, such as  $\text{Nd}_{2-x}\text{Ce}_x\text{CuO}_4$  (NCCO)<sup>53</sup>, is still a controversial topic<sup>14,21,23,24,54,55</sup>.

Here, we argue that pairing symmetry in cuprate superconductors may also be explained analytically in the picture of the real space Coulomb confinement effect of Fig. 4. In the case of hole-doped copper oxides, as shown in Fig. 4, the pair with  $\mathbf{M}_s$  parallel to  $x$ - and

$y$ -axis has a minimum  $\Delta(\theta)$  that leads to a maximum binding energy of Eq. (4), namely, the maximum energy gap in these four directions. Furthermore, it is possible that the pair ( $\mathbf{M}_s$  along the diagonal directions) can be destroyed [ $\Delta(\theta) > \sqrt{2}a$ ] due to the strong Coulombic interaction between the pair and ions  $\text{Cu}^{2+}$ , hence, the corresponding binding energies may be zero in these four directions. Within the proposed real-space confinement mechanism, the pairing picture for the electron-doped systems is remarkably similar to that of the hole-doped cuprates, with one major difference comes from the substitution of  $\text{O}^{1-}$  by  $\text{O}^{2-}$  (see also Fig. 4). This substitution, on the one hand, greatly enhance the confinement effect by increasing  $F_1$  in (100), (010),  $(\bar{1}00)$  and  $(0\bar{1}0)$  directions and in turn will shorten the distance  $\Delta(\theta)$  and increase the binding energy, on the other hand, it can greatly reduce the possibility of the “pair-breaking” along directions (110),  $(\bar{1}10)$ ,  $(\bar{1}\bar{1}0)$  and  $(1\bar{1}0)$ , in other words, now the diagonal’s pair is more likely to survive in the electron-doped cuprates than in the hole-doped cuprates. Roughly speaking, our unified model for cuprate superconductivity yields for the hole-doped ( $p$ -type) and electron-doped ( $n$ -type) cuprates to have essentially the same pairing mechanisms, but different spatial pairing symmetries.

To make the arguments of pairing symmetry more convincing, below more detailed studies will be done based on the simple Coulomb’s equation. As shown in Fig. 4, in the case of the nearest-neighbor (marked by 1, 2, 3, 4) and next-nearest-neighbor interactions (marked by 5, 6, 7, 8), the forces acting on (push/pull) the pair are in eight different directions. Within this framework, the pair will stay at the most unstable state in the pair’s orientation due to the strong repulsive Coulomb interaction between the two electrons in this direction, we are therefore paying particular attention to the confinement effect in the same direction as the orientation of the pair. If the electron pair is oriented in  $x$ - and  $y$ -axis or the diagonal directions, because of the structural symmetry, we can present the explicit analytical expressions of the confinement effects. Figures 5(a) and (b) illustrate the eight Coulombic forces and the total confinement forces [ $F^\eta(100)$ ,  $F^\eta(110)$ ] exerted on the two electrons of the pair in (100) and (110) directions of the cuprate samples, respectively. It is easy to have some similar figures in other directions for both  $p$ -type and  $n$ -type superconductors. According to Fig. 5, we can get a general formula of the total confinement force  $F^\eta(100)$  applied to the electron of the pair in (100) direction as

$$F^\eta(100) = \frac{e^2}{4\pi\epsilon_0} \left[ \eta \left( \frac{1}{d_1^2} - \frac{1}{d_2^2} \right) + \frac{1}{d_3^2} - \frac{1}{d_4^2} \right], \quad (5)$$

where  $\eta = 1$  for hole-doped case, while  $\eta = 2$  for electron-doped cuprates. And the parameters  $d_1$ ,  $d_2$ ,  $d_3$  and  $d_4$

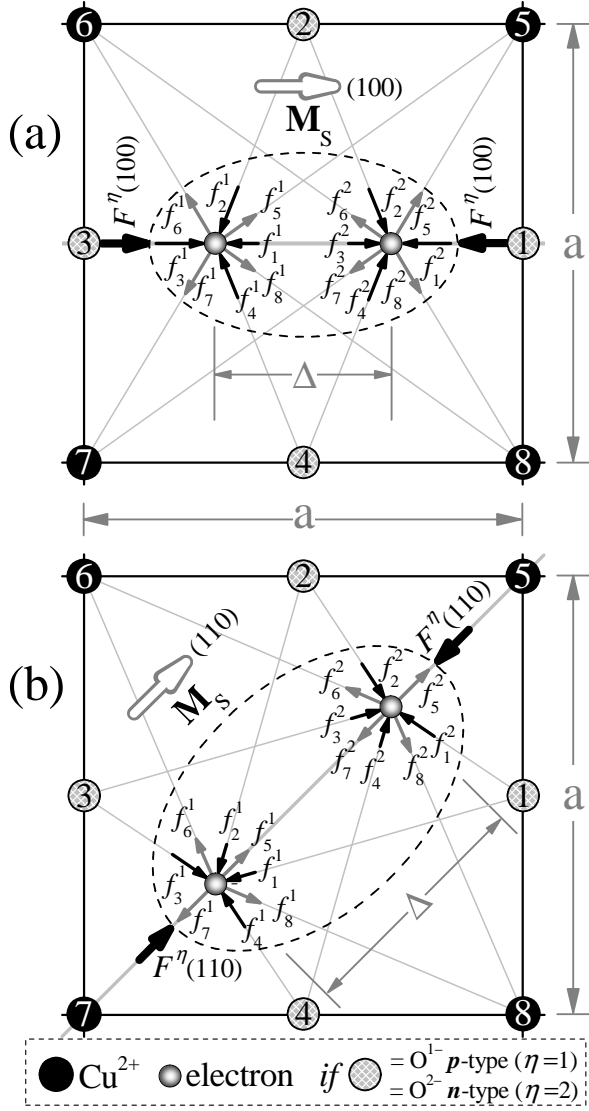


FIG. 5: The schematic plot of the confinement forces acting the electron pair inside one unit cell of the CuO plane. The pair oriented ( $\mathbf{M}_s$ ) in (a) (100) direction ( $\theta = 0$ ), and (b) (110) direction ( $\theta = \pi/4$ ).

are defined by

$$d_1 = \frac{\sqrt{a^2 - \Delta^2}}{4\sqrt{a\Delta}}, \quad d_2 = \frac{(a^2 + \Delta^2)^{3/4}}{2\sqrt{2}\Delta},$$

$$d_3 = \frac{(2a^2 + \Delta^2 + 2a\Delta)^{1/4} \sqrt{2a^2 + \Delta^2 + \sqrt{2}a\Delta}}{4\sqrt{a + \Delta}},$$

$$d_4 = \frac{(2a^2 + \Delta^2 - 2a\Delta)^{1/4} \sqrt{2a^2 + \Delta^2 - \sqrt{2}a\Delta}}{4\sqrt{a - \Delta}},$$

where  $\Delta < a$ . Similarly, in (110) direction, we have

$$F^\eta(110) = \frac{e^2}{4\pi\epsilon_0} \left[ \frac{1}{D_1^2} - \frac{1}{D_2^2} + \eta \left( \frac{1}{D_3^2} - \frac{1}{D_4^2} \right) \right]. \quad (6)$$

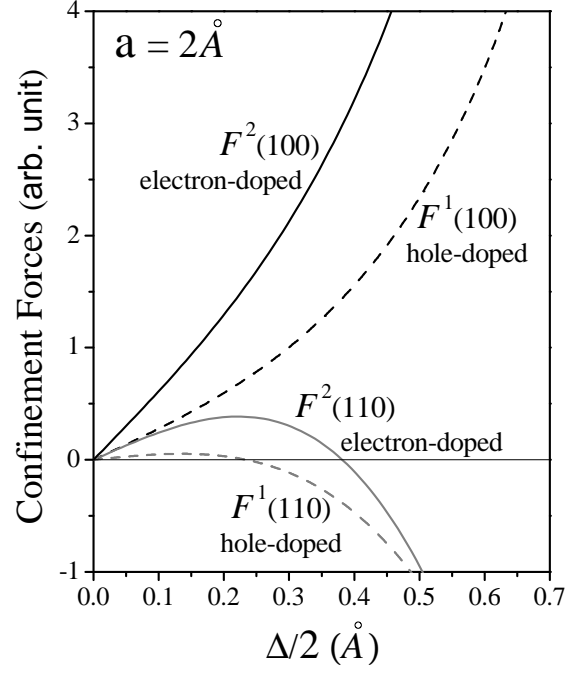


FIG. 6: Analytical confinement forces versus  $\Delta/2$  in electron- and hole-doped cuprate superconductors along (110) and (100) directions. In the case of electron doping (solid lines), when  $\Delta$  is small, both confinement forces in (110) and (100) are positive, but note that (100) confinement (black solid line) is stronger than (110) confinement (gray solid line), these yield the ( $s + d$ ) symmetry in the system. In the case of hole doping (dashed lines), for a small  $\Delta$ , there is a strong confinement in (100) direction (black dashed line), while a very weak confinement in (110) direction (gray dashed line), these results indicate a dominating  $d$ -wave pairing symmetry (with a small  $s$ -wave component) in hole-doped cuprates.

Here too  $\eta = 1$  and  $\eta = 2$  for hole- and electron-doped cuprates, respectively. The four distance parameters in Eq. (6) are given by

$$D_1 = \frac{(2a^2 + \Delta^2)^{3/4}}{4\sqrt{\Delta}}, \quad D_2 = \frac{(2a^2 - \Delta^2)}{4 \times 2^{3/4} \sqrt{a\Delta}},$$

$$D_3 = \frac{(a^2 + \Delta^2 - \sqrt{2}a\Delta)^{3/4}}{2\sqrt{\sqrt{2}a - 2\Delta}},$$

$$D_4 = \frac{(a^2 + \Delta^2 + \sqrt{2}a\Delta)^{3/4}}{2\sqrt{\sqrt{2}a + 2\Delta}},$$

where  $\Delta < a/\sqrt{2}$ .

From equations (5) and (6), if  $F^\eta(100) > 0$ , the total confinement is “positive” and the pair tends to be stable in (100)-(100) directions, while  $F^\eta(100) < 0$ , the total confinement is “negative” and the pair with an apparent tendency to be broken up in these directions. Thus the situation is the same as for the  $F^\eta(110)$ . With the analytical expressions (5) and (6), we draw in Fig. 6 the confinement forces versus  $\Delta/2$  (two solid lines for

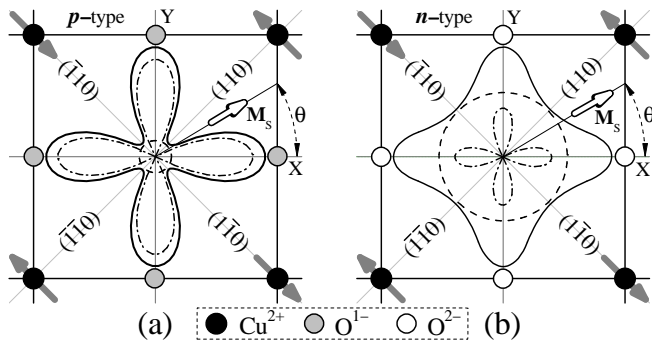


FIG. 7: Pairing symmetry in cuprate superconductors, (a) hole-doped, (b) electron-doped. The pairing electrons maintain their integrity inside the single plaquette with the dominant  $d$ -wave (a mixture of large  $d$ -wave and small  $s$ -wave components) and  $(s+d)$ -wave symmetry in  $p$ -type and  $n$ -type samples, respectively.

electron-doped case, while the dash lines for hole-doped sample) under the condition  $a = 2\text{\AA}$ . This figure reveals three important facts: (i) in the case of hole doping, the existence of a strong confinement in (100) direction as expected, a surprising result is that, there is a very weak confinement in (110) direction; (ii) in the case of electron doping, if  $\Delta/2 \leq 0.38\text{\AA}$ , both confinement forces in (110) and (100) are positive, but note that (100) confinement is stronger than (110) confinement, (iii) in both cases (hole and electron doping), the net confinement  $F^\eta(100)$  is always positive inside the unit cell. Having obtained the strongest confinement  $F^\eta(100)$  and the weakest confinement  $F^\eta(110)$  for both hole- and electron-doped cuprates (see Fig. 6), now we can qualitatively determine the pairing symmetries for two different doped systems, as shown in Fig. 7. The solid black curve of Fig. 7(a) shows a mixture of large  $d$ -wave (dash-dotted curve) and small  $s$ -wave (dashed circle) pairing symmetries in hole-doped cuprates. Our theoretical result of Fig. 7(a) is in satisfactory agreement with the experiments indicating the existence of a very small  $s$ -wave component in hole-doped cuprates<sup>56,57</sup> Also, basing on the Fig. 6, the results definitely favor the  $(s+d)$  symmetry in electron-doped cuprates, as shown in Fig. 7(b).

In fact, the above discussions have been restricted to the idealized condition of zero temperature. If temperature induced thermal effects (lattice vibration) are taken into account, the obvious difference [Fig. 7(a) and (b)] in pairing symmetry between hole- and electron-doped cuprates can be further interpreted from the viewpoint of the superconducting transition temperature  $T_c$ . It is well known that the maximum  $T_c$  in the hole-doped cuprates is  $133\text{ K}$ , which is much higher than that of the electron-doped systems (about  $30\text{ K}$ ), for this reason, a larger dynamical local lattice distortion in the CuO plane can be expected in the hole-doped cuprates. As a result, the electron pair is more likely to be broken up by ions  $\text{Cu}^{2+}$  along the diagonal directions of Fig. 7(a), this discus-

sion provides a further support the predominantly  $d$ -wave superconducting symmetry in the hole-doped cuprates. Lowering the cuprates temperature will possibly result in a symmetry transition from  $d$ -wave to  $(s+d)$ -wave in hole-doped systems. We think the suggested scenario offers a new way for physical interpretation of the pairing symmetry in the cuprates.

### C. Pseudogap in the cuprate superconductors

The nature of the normal-state gap (pseudogap) phase of HTSC is also highly controversial<sup>158,59,60,61,62,63,64</sup>. ARPES and tunneling measurements show a clear pseudogap which was seen to persist even at room temperature<sup>25,61,63</sup>. There are many models attempt to describe the mysterious pseudogap state. Strictly speaking, none of the proposed models is completely satisfactory. As discussion above, here we present a new approach based on the simple and natural picture of the real-space confinement effect, and the pseudogap is associated with the local structure of unit cell in  $\text{CuO}_2$  plane. Thus it should not be surprising about the pseudogap behavior which indicate the formation of pairs below  $T^* > T_c$ . The real space Coulomb confinement picture (see Fig. 4) shows clearly that the pair is confined within one single plaquette, consequently, the “size” of the electron pair [distance  $\Delta(\theta)$ ] is much less than one lattice constant. For  $\Delta(\theta) < 0.22\text{\AA}$ , the binding energy of Eq. (4) may be much larger than the magnetic Heisenberg exchange ( $J \sim 0.1\text{eV}$ ). This support the experiments that the pseudogap can exist in the cuprate superconductors at a temperature even higher than room temperature.

The presence of pseudogap in underdoped cuprate superconductors has been a solid experimental fact. However, whether it is a continuation of the superconducting gap as a result of pre-formed pairs is a topic of current debate. Our results suggest that the pseudogap is a general feature of all transition metal oxides, not just cuprate superconductors. The newly observations of the Cooper pair localization in the amorphous insulating systems<sup>11</sup>, in fact, reveal that pair correlations may be built up in the real space confinement screening and the pseudogap is a common feature in nature materials that is consistent with our arguments in this section.

## IV. CRYSTALLINE ELECTRON PAIRS, CHARGE STRIPES AND SPIN DENSITY WAVE

Physically, pairing in cuprates is an individual behavior characterized by pseudogap, while superconductivity is a collective behavior of many coherent electron pairs. Nowadays, more and more beautiful experimental results suggest that stripes are common in cuprates and may be important in the mechanism for HTSC<sup>10,29,30,39,46,65,66,67,68,69,70,71</sup>. Here, we argue that there are only two specific stripes which would contribute

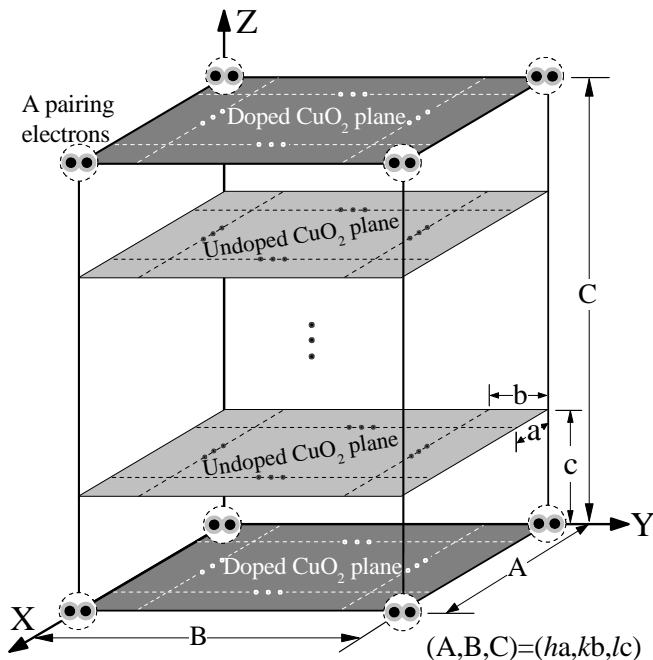


FIG. 8: Simplified schematic unitcell of the electron-pairs (dimerized) Wigner crystal in the high- $T_c$  cuprates.

to the mechanism of superconductivity in cuprate superconductors and the dynamical spin density wave (SDW) coherent phases can be established along the stripes.

### A. Wigner crystal and charge stripes

In nature, periodic structures are often considered as the result of competition between different interactions. The formation of stripe patterns is generally attributed to the competition between short-range attractive forces and long-range repulsive forces<sup>72</sup>. Obviously, our scenario provides not only the “glue” for the electron pairs but also the most basic competitive environment [attraction  $F_m$  of Eq. (2) and repulsion  $F_e$  of Eq. (1) among the electron pairs] for the possible formation of charge stripe. In this paper, we focus on the doping-induced behaviors of  $\text{La}_{2-x}\text{Sr}_x\text{CuO}_4$  with the primitive cell  $(a, b, c)$ . At a rather low doping level, the interactions among electron pairs can be neglected and the superconductor behaves much like a charged random system. However, as more carriers are added, the effect of the competitive interactions among electron pairs will emerge. As a result, at a proper doping level the electron pairs can self-organize into a ‘superlattice’ (Wigner crystal of electron pairs) with the primitive cell  $(A, B, C) = (ha, kb, lc)$ , as shown in Fig. 8. Consequently, the “material” composed of electron-pair “atoms” will undergo a structure transition from random to order phase (LTO or LTT). Thus, the carrier density  $x$  is given by

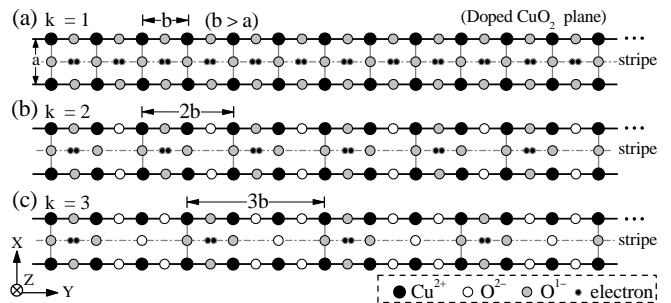


FIG. 9: The quasi-one-dimensional charge stripes in high- $T_c$  cuprates, (a) and (b) are the metallic charge stripes, where the central chains are composed of mono-ion ( $\text{O}^{1-}$ ), while (c), the insulating charge stripe, there are two different ions ( $\text{Cu}^{2+}$  and  $\text{O}^{1-}$ ) in the central chain.

$$x = p(h, k, l) = 2 \times \frac{1}{h} \times \frac{1}{k} \times \frac{1}{l}, \quad (7)$$

where  $h$ ,  $k$ , and  $l$  are integral numbers. As can be seen, the ‘superlattice’ scheme is most consistent with the recent experimental observations of the two-dimensional nature of the charge stripes<sup>39,73,74</sup>. Expression (7) plays a key role in the following studies.

When the charge stripe spacing satisfying  $A \gg B$ , the quasi-one-dimensional striped phase can be expected<sup>46,65,66</sup>. In this case, we can devote most of our attention to the ladder structures of Fig. 9. One particularly important conclusion can be drawn from this figure. When  $k = 1$  or  $2$ , inside the ladder [Fig. 9(a) and (b)] there is an perfect mono-ion ( $\text{O}^{1-}$ ) chain where the coherence can be easily established among electron pairs, hence the corresponding charge stripes are metallic. In fact, the new type of orders of Fig. 9(a) and (b) show the typical case of a charge-Peierls dimerized transition. As shown in Fig. 9(c), while for  $k \geq 3$ , the middle chain is now impure (containing two kinds of oxygen ions  $\text{O}^{1-}$  and  $\text{O}^{2-}$ ) and this will greatly restrain the establishment of coherence among electron pairs, as a result the strips will behave more like the one-dimensional insulators<sup>46,65</sup>. It appears, then, that the pure and perfect oxygen ion ( $\text{O}^{1-}$ ) chains inside the charge stripes play a central role in the superconductivity. In addition, the one-dimensional nature (the charge stripes extend along  $b$ ) indicates that the Coulombic interactions between two nearest neighbor electron pairs along the  $b$  direction is much stronger than that of electron pairs along  $a$ , then the anisotropic lattices ( $b > a$ ) should be found experimentally in the  $\text{CuO}_2$  plane<sup>1,75</sup>.

### B. Spin density wave (SDW)

Currently, the magnetic (spin) excitation has been observed by neutron scattering in a number of hole-



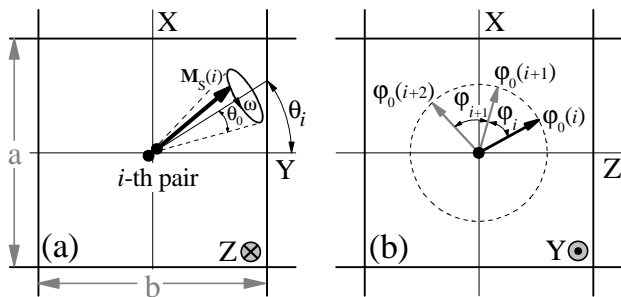


FIG. 10: The initial magnetic phase relationship of the electron pairs in the charge stripe of Fig. 9(a). (a) The  $i$ -th electron pair with  $\mathbf{M}_s(i)$  is oriented at angle  $\theta_i$  and  $\theta_0$  corresponds to a small-angle precession (fluctuations) due to the thermal vibrations of the lattices, (b) the initial magnetic phase difference between two nearest-neighbor pairs. In the non-superconductivity state,  $\theta_i$  and  $\varphi_i$  are random; while in superconductivity state,  $\theta_i$  and  $\varphi_i$  will correspond to a constant, respectively.

doped<sup>76,77,78,79</sup> and electron-doped materials<sup>80,81</sup>. It is generally believed that magnetic excitations might play a fundamental role in the superconducting mechanism. Our results above demonstrate that the short-range real space electron-electron interactions are relevant to the pairing symmetry (pseudogap) and we would expect in the following that the magnetic interactions (magnetic resonance) among electron pairs is essential in the mechanism of superconductivity. It should be noted that Fig. 9 is merely a schematic picture which is by no means a complete restriction of the stripes in the center of ladders. Evidently, a direct interaction among electron pairs and the domain-walls ( $\text{Cu}^{2+}-\text{O}^{1-}$  chains for  $k=1$ ) will result in the fluctuations of stripes which have been confirmed by experiments<sup>46,65,66,68</sup>.

It is well known that the concept of the superconducting order parameter, which was first introduced by Ginzburg and Landau (GL)<sup>82</sup> in their study of the superconducting state in 1950, is a very important factor for the qualitatively description of the ordered state of various phase transitions. To describe the competition between superconductivity and charge stripe order in Fig. 9, based on the GL theory formalism, a complex position-dependent order parameter can be defined as

$$\Psi = \Lambda e^{i\Phi},$$

and parameters  $\Lambda$  and  $\Phi$  are

$$\Lambda = \frac{1}{n} \sum_i \mathbf{M}_s(i),$$

$$\Phi = \frac{1}{n} \sum_i [\varphi_0(i+1) - \varphi_0(i)] = \frac{1}{n} \sum_i \varphi_i,$$

where  $\mathbf{M}_s(i)$  is the joint magnetic moment of the  $i$ -th electron pair, and  $\varphi_0(i)$  and  $\varphi_i$  are the initial phase and

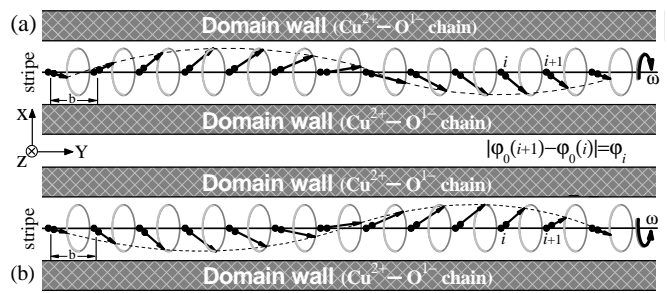


FIG. 11: Due to the magnetic phase-coherence (the initial phase difference  $\varphi_i = \varphi_0$  is a constant) among the electron pairs, a helical dynamical spin-density-wave (DSDW) is inspired in the metallic charge stripe of Fig. 9(a) and the superconductivity and DSDW can coexist along this stripe, (a) The left-hand SDW, and (b) the right-hand SDW. Similar dynamical SDW can also exist in Fig. 9(b).

the initial phase difference between two nearest-neighbor pairs (see Fig. 10), respectively. As shown in Fig. 10(a), the  $\mathbf{M}_s(i)$  is oriented at angle  $\theta_i$  and  $\theta_0$  corresponds to a small-angle precession due to the following two reasons: (i) a short-range magnetic interaction between the  $\mathbf{M}_s(i)$  and antiferromagnetic background of  $\text{CuO}$  plane; (ii) the thermal vibrations of the lattices. Fig. 10(b) shows the initial phases and the initial phase differences of the phase-incoherent electron pairs inside the charge stripe of Fig. 9(a). Without an external field,  $\theta_i$  and  $\varphi_i$  are random, hence  $\Lambda$ ,  $\Phi$  and the order parameter  $\Psi$  are zero. In such a situation, although all electrons may have been paired under appropriate temperature  $T^*$ , they are completely incoherent and the superconductivity might not be expected in the charge stripes. When  $T < T_c$  and an external field is applied (for example, in  $y$ -direction) to the cuprate sample, in this case  $\theta_i = 0$ ,  $\theta_0 \neq 0$  and  $\varphi_i = \varphi_0$  is a constant, then  $\Lambda$ ,  $\Phi$  and  $\Psi$  reach their maximum values, indicating the occurrence of symmetry breaking and the superconductive transition. As a result, a real space helical dynamical spin-density-wave (SDW) (segregated by the domain wall) and superconductivity coexist to form a supersolid, as shown in Fig. 11. Therefore, if stripes are to have a positive relevance to superconductivity in the cuprates, then they must be able to exist in a dynamic magnetic coherent form. It is obvious that a similar superconductive stripe phase can occur in Fig. 9(b). Now, the real space helical SDW is proved to be a much richer natural phenomenon<sup>83</sup>, not restricted to cuprate superconductors.

## V. MAGIC DOPING FRACTIONS

In fact, one particularly important characteristic of the HTSC is the competition among different order phases. This competition could emerge as a result of some intriguing features such as the “magic doping fractions” in

high- $T_c$  superconductors<sup>38</sup>. It is of much interest to note that our mechanism offers a natural explanation of the physical origin of these observations<sup>39,46,65,66,73,74</sup>. Generally, the “superlattice” (electron pairs) exist in LTO phases. In this paper, it is argued that the “magic doping phases” in cuprates can exist in the LTT “superlattice” phases. Moreover, it is shown that there are two different kinds of LTT “superlattice” phases: LTT1 phases (where  $A = B \neq C$  and  $a = b$ ), in which the square superstructure of electron pairs is inside the  $\text{CuO}_2$  plane; LTT2 phases (where  $B \ll A = C$  and  $b > a$ ), in which the square superstructure is perpendicular to the  $\text{CuO}_2$  plane. Further studies indicate that the LTT1 phases are related to the anomalous suppression of superconductivity, while the LTT2 phases would contribute to the mechanism of superconductivity in cuprate superconductors.

### A. Underdoped ( $x = 1/18, 1/8, 1/16, 1/9$ )

The experimental and theoretical results demonstrate that the insulator-to-superconductor transition in the underdoped regime ( $x \approx 0.055$ ) in LSCO<sup>68,69,70,84</sup>. We note that the observed decimal number (0.055) is coincident with a rational doping level ( $\sim 1/18$ ). At  $x = 1/18$ , there are some possible configurations, [for instance,  $p(6, 6, 1)$ ,  $p(6, 3, 2)$ ,  $p(12, 1, 3)$ ,  $p(18, 1, 2) \dots$ ], which satisfy Eq. (7). From the viewpoint of the stripe stability, the charge orders tend to choose the LTT1 phase of  $p(6, 6, 1)$  and the corresponding doped  $\text{CuO}_2$  plane is shown in Fig. 12(a). It can be seen from this figure that all the paired electrons are localized at the lattice points of the superlattice and thereby hinder the superconductivity. At  $x = 1/8$ , another LTT1 “superlattice” phase of  $p(4, 4, 1)$  can also coexist with the LTT original lattice ( $a = b$ ) of the LSCO [see Fig. 12(b)]. This may explain the famous “1/8 anomaly” in various high- $T_c$  superconductors<sup>29,37,85,86,87,88</sup>. At the doping level 1/8, results of recent STM experiments on  $\text{Bi}_2\text{Sr}_2\text{CaCu}_2\text{O}_x$  (BSCCO)<sup>67</sup> and  $\text{Ca}_{2-x}\text{Na}_x\text{CuO}_2\text{Cl}_2$  (CNCOC)<sup>10</sup> suggest a checkerboard-like spatial modulation of electronic density of states with a periodicity of  $4a \times 4a$ . Several theoretical scenarios have been proposed to explain the commensuration charge ordering patterns<sup>10,38,49,89,90</sup>. We consider that the schematic [Fig. 8 and Eq. (7)] is a promising approach to the problem, as it can explain the longstanding puzzle in a very natural way.

Specifically, we find that this simple picture can provide some preliminary evidence for the other anomalous behaviors in cuprates. From Eq. (7), it is clear that the nondispersive superlattices of  $4a \times 4a$  and  $3a \times 3a$  in  $\text{CuO}_2$  planes can be expected at  $x = 1/16$  (see Kim *et al.* for details)<sup>39</sup> of  $p(4, 4, 2)$  and  $x = 1/9$  of  $p(3, 3, 2)$ , respectively. Therefore, the anomalous suppression of the superconductivity can be found in LSCO at  $x = 1/9$  and  $x = 1/16$ . Encouragingly, some unusual results have already been observed at  $x = 1/16$  and  $x = 1/9$  of the underdoped LSCO crystals. For instance, by high resolu-

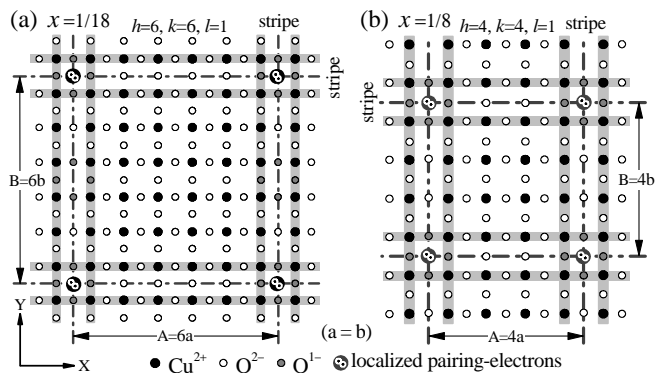


FIG. 12: The nondispersive superlattices of the electron pairs in the doped  $\text{CuO}_2$  planes. (a)  $x = 1/18$ , and (b)  $x = 1/8$ . Both the superlattice of electron pairs and the original lattice are in the LTT phase, especially the superstructures with a commensurate periodicity of lattice constants are formed within the Cu-O planes.

tion ARPES experiments on  $x \sim 1/16$  sample, an anomalous change at  $\sim 70$  meV in the nodal scattering rate was reported<sup>40</sup>, and the observations of intrinsic anomalous superconducting properties at magic doping levels of  $x = 1/16$  and  $x = 1/9$  had been found by *dc* magnetic measurements<sup>41</sup>. It is important to mention that the present results well explain an open question: why two different LSCO compounds ( $x = 1/8$  and  $x = 1/16$ ) can exhibit the same nondispersive  $4a \times 4a$  superstructure within their  $\text{CuO}_2$  planes.

Neutron scattering provides a direct measure of the magnetic excitation spectrum. High resolution neutron scattering experiments on optimally doped  $\text{La}_{2-x}\text{Sr}_x\text{CuO}_4$  ( $x = 0.16$ )<sup>73</sup> and  $\text{YBa}_2\text{Cu}_3\text{O}_{6+x}$ <sup>91</sup> reveal that the magnetic excitations are dispersive. However, a similar study on  $\text{La}_{2-x}\text{Ba}_x\text{CuO}_4$  ( $x = 1/8$ ) shows some nondispersive superlattice peaks indicative of spin and charge stripe order<sup>88</sup>. In particular, in  $\text{La}_{1.6-x}\text{Nd}_{0.4}\text{Sr}_x\text{CuO}_4$  for  $x = 1/8$ , the static SDW and charge-density-wave (CDW) have been discovered<sup>29</sup>. The same observations have been reported in other cuprates<sup>68,88,92</sup>. Note that the static SDW and static CDW, which are bad for superconductivity, are very different from the dynamic SDW (see Fig. 11) which is good for superconductivity. Several possible mechanisms have been proposed to explain these observations<sup>35,93,94,95,96,97</sup>. It is argued that the nature of the spin order may not be directly related to the nature of the charge order, which can be regarded as a result of spin-charge separated scheme<sup>2</sup>. But we consider that a real description of superconducting electrons should be the charge-“spin”-binding picture: charge dimerized and “spin” coherent. As shown in Fig. 12, we have very strong insulating phases which correspond to some ordering charge stripes of simple checkerboard patterns of electron pairs. This static ordering of stripes may explain why superconductivity disappears close to these fillings.

Moreover the schematic superlattice structure of Fig. 8, a new charge-“spin” binding picture, suggests that the confining magnetic interactions among the pairs can also inspire the static SDW and CDW at the same time. As observed in experiments, the static stripes are in fact in motion<sup>68</sup>.

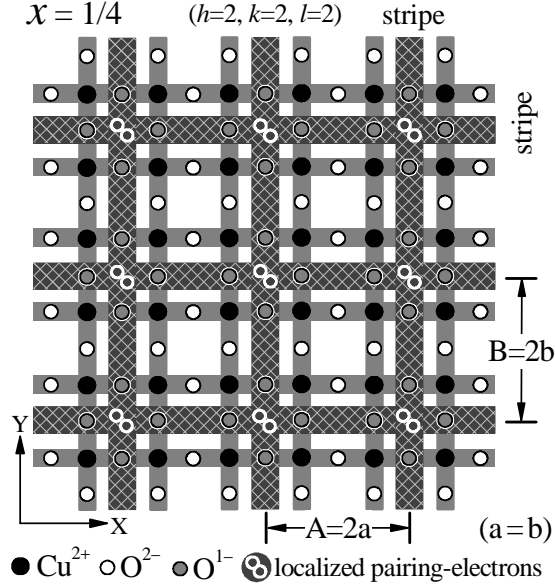


FIG. 13: Similar to the underdoped cases of Fig. 12, the rotationally symmetric charge periodicity of  $2a \times 2a$  is inside the  $\text{CuO}_2$  plane of the overdoped LSCO at  $x = 1/4$ .

### B. Overdoped ( $x = 1/4$ )

In contrast to the various and complicated physical phenomena in the underdoped region, the electronic behavior in the heavy-doped samples (overdoped) appear to be very simple. It is commonly believed that an ordering of paired electrons can be formed in the LSCO exhibiting the anomalous properties in the overdoped region. Spin excitations and transport properties of LSCO in the overdoped regime have been investigated in detail, anomalously less-metallic behaviors of the electrical resistivity and the thermoelectric power have been found in the materials. In particular, experimental verification of the strong-correlation fluctuations in a non-superconductive  $x = 1/4$  sample has been noted<sup>98</sup>. Most recently, Wakimoto *et al.*<sup>99</sup> reported the structural and neutron-scattering experiment study for over-doped LSCO with  $x = 1/4$ . They confirmed that the crystal structure of the composition has tetragonal symmetry (LTT1 phase) with lattice constant of  $a = b = 3.73 \text{ \AA}$  at 10 K and the IC peaks appear around the antiferromagnetic wave vector  $(1/2, 1/2)$ . These interesting observations can be well understood via Eq. (7), which indicates that there exists only one possible LTT1 superlattice phase within this

region. As shown in Fig. 13, this phase has a rotationally symmetric charge periodicity of  $2a \times 2a$  at  $x = 1/4$  of  $p(2, 2, 2)$ . Accordingly, no superconductivity has been observed at the  $x = 1/4$  and even higher doping levels.

It should be noted that our analytical predictions in overdoped region are also found to be in excellent agreement with the experimental data. This fact would add considerable support that our theory has the great merit of explaining high- $T_c$  superconductivity.

### C. Stable superconducting phase ( $x = 1/7, 1/14$ ) and optimal doping

Since the pioneering experiments of Bednorz and Müller<sup>1</sup>, the structure and physical properties have been extensively investigated on the optimally doped LSCO<sup>8,54,59,100,101</sup>. It is commonly accepted that samples of  $\text{La}_{2-x}\text{Sr}_x\text{CuO}_4$  have the highest  $T_c$  at Sr concentration (optimal doping)  $x \sim 1.51$  with the experimental lattice constants:  $a = 3.788 \text{ \AA}$  and  $c = 13.25 \text{ \AA}$ . In this subsection, basing on the Fig. 9 and Fig. 11, we will attempt to provide a general description of the stable superconducting phase (metallic stripe) in LSCO and give a possible relationship between the stable doping phase and optimal doping phase.

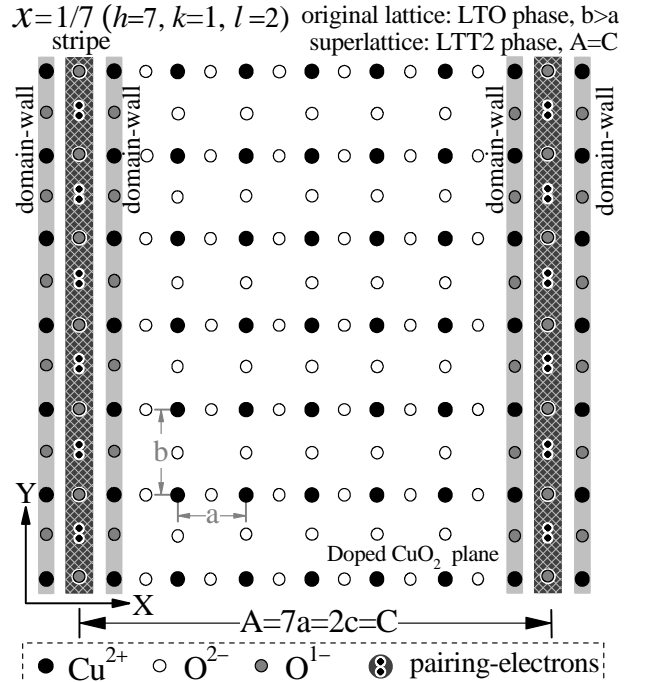


FIG. 14: A stable superconducting stripe order in the  $\text{CuO}_2$  plane at  $x = 1/7$ , which is near the optimal doping. The charge stripes are segregated by the domain walls of  $\text{Cu}^{2+}-\text{O}^{1-}$  chain. However, unlike Fig. 12 and Fig. 13, here the square superlattice structure is in the plane perpendicular to the  $\text{CuO}_2$  plane.

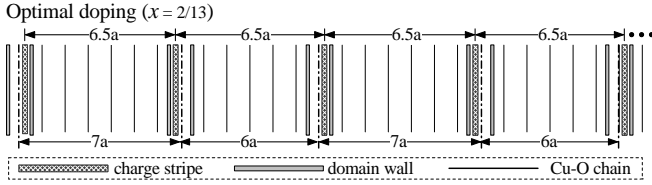


FIG. 15: A possible mixed phase in LSCO with the optimal doping  $x = 2/13 \approx 1.53$ .

From these structure parameters, then one has  $7a (\sim 26.516\text{\AA}) \approx 2c (\sim 26.5\text{\AA})$  which may possibly relate to the optimally-doped. When  $7a = 2c$  ( $x = 1/7 \approx 0.143$ ), the coexistence of a stable LTT2 superconductive superlattice phase of  $p(7, 1, 2)$  and the LTO original lattice ( $b > a$ ) of the LSCO is shown in Fig. 14. However, the analytical value of the optimal doping density ( $\sim 0.143$ ) is slightly lower than that obtained through the experimental studies. We argue that the physically significant critical value for the stable superconducting phase is not that at which  $T_c$  is maximum. As shown in Fig. 15, the maximum high- $T_c$  phase may be relevant to a LTT2 related metastable superconducting phase, for example, a uniform mixture of  $x = 1/7$  and  $x = 1/6$  with an optimal doping at  $x \sim 1.53$ . In addition, recall that another possible superconducting stripe (metallic) is shown schematically in Fig. 9(b), under the restriction of  $7a = 2c$ , one can also find another stable superconducting stripe phase at  $x = 1/14$  of  $p(7, 2, 2)$ .

## VI. PHASE DIAGRAM AND SUPERCONDUCTIVE CRITERION

For the discussion of our results, we summarize the doping dependence of  $T_c$  for LSCO in a schematic phase diagram in Fig. 16. It is well known that the antiferromagnetic Mott insulator phase is found near the origin of  $\text{La}_2\text{CuO}_4$ . For doping beyond a few percent, the material enters the disordered phase (spin glass). At  $x = 1/18$ , the material will undergo an insulator-to-metal transition, at the same time displaying superconductivity at low temperature. According to Eq. (7), the “magic effect”<sup>85</sup> is possibly taking place at rational doping levels  $1/4$ ,  $1/8$ ,  $1/9$ ,  $1/16$  and  $1/18$ , where the LTT1 superlattice phases ( $A = B$ ) can coexist with the LTT original lattices ( $a = b$ ) in the LSCO. In these specific situations, the paired electrons are localized, hence the corresponding charge orders appear to be completely destructive to superconductivity.

We note here that the bosonic theory predicts all magic doping fractions at  $x = (2m + 1)/2^n$ , where  $m$  and  $n$  are integers<sup>38</sup>, which implies the possibility of an infinite magic doping fractions in LSCO, while our theory predicts commensurate effect only at five magic doping fractions  $1/4$ ,  $1/8$ ,  $1/9$ ,  $1/16$  and  $1/18$  (see Fig. 16). The

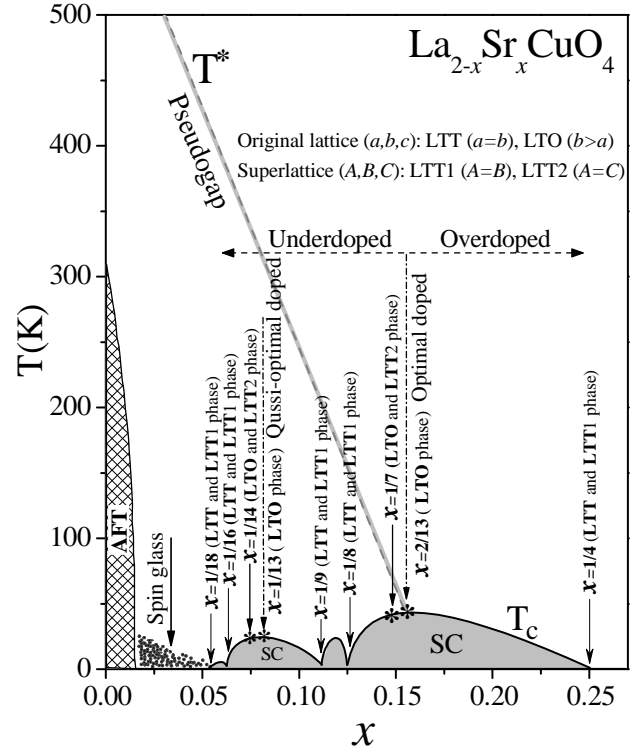


FIG. 16: An analytical phase diagram for LSCO. There are five abnormal phases (at  $x = 1/4$ ,  $1/8$ ,  $1/9$ ,  $1/16$  and  $1/18$ ), where the LTT1 superlattice phases ( $A = B$ ) can coexist with the LTT original lattices ( $a = b$ ) in the LSCO.

reported measurements find a tendency towards charge ordering at five particular rational doping fractions of  $1/4$ <sup>99</sup>,  $1/8$ <sup>29,85,86,87,88</sup>,  $1/9$ <sup>40,41</sup>,  $1/16$ <sup>39</sup> and  $1/18$ <sup>68,69,70,84</sup> and is most consistent with our theoretical prediction. In view of the intriguing agreement of the experimental data with our model, it would be desirable to systematically perform direct measurements of the charge order in the underdoped LSCO materials, where the nondispersive checkerboard-type ordering with periodicity  $3a \times 3a$  and  $6a \times 6a$  can be experimentally observed at the doping levels  $x = 1/9$  and  $1/18$ , respectively.

While at  $x = 1/7$  and  $x = 1/14$ , due to the relation  $2c = 7a$  in LSCO, the quasi-one-dimensional metallic charge stripe orders [see Fig. 9(a) and (b)] can coexist with superconductivity. In particular, our results imply that the emerging of the superconductivity in high- $T_c$  cuprates is always accompanied by the distortions of the original lattice (a transition from LTO to LTT phase) in  $\text{CuO}_2$  planes. Thus, the following ratio of the lattice constants

$$\delta = \frac{b - a}{a}, \quad (8)$$

where  $b \geq a$ , can be used to interpret qualitatively the behavior of the HTSC. When  $\delta = 0$  (or  $b = a$ ), the superconductivity is totally suppressed by the stable charge stripes (the square patterns formed inside the

CuO<sub>2</sub> planes). While  $\delta = \delta_{\max}$ , the superconductivity will be enhanced greatly by the anisotropy charge stripes in the  $a - b$  plane and the corresponding value  $x$  appears to be the optimal doping.

## VII. CONCLUDING REMARKS AND FURTHER EXPERIMENTS

In conclusion, we have shown a complete replacement of the concept of quasi-particles (holes) by the real electrons, giving rise to a quite different electronic pairing and superconductive mechanism. We have found that two localized electrons can bind together by the photon-mediated electromagnetic interaction. Our model favors the dominant  $d$ -wave symmetry in hole-doped cuprates. In the electron-doped cuprate, the result suggests a possible mixed ( $s + d$ )-wave symmetry.

At an appropriate low temperature and doping level, we show that paired electrons can self-organize into the so-called dimerized Wigner crystal. Remarkably, two kinds of quasi-one-dimensional metallic magnetic-charge stripes, where the superconductivity and dynamical spin density wave (SDW) coexist, have been analytically and uniquely given. Furthermore, the mechanism has predicted theoretically the “magic effect”<sup>85</sup> at rational doping levels  $1/4$ ,  $1/8$ ,  $1/9$ ,  $1/16$  and  $1/18$  in LSCO. Our results have provided a vivid physical picture which illustrates clearly how the stripes compete with superconductivity in high- $T_c$  cuprates. Besides, we have presented for LSCO an analytical phase diagram which is in satisfactory agreement with the observations from experiments. In fact, the important theoretical<sup>12</sup> and experimental<sup>11</sup> results imply that the famous BCS theory<sup>9</sup> may be incorrect. Hence, we argue that the any electronic pairing phenomena should share exactly the same pairing mechanism. The basic idea of the present paper may also proved to be important for any other superconductors, for instance, the conventional superconductors, MgB<sub>2</sub><sup>102</sup>, and organic superconductors<sup>103</sup>.

As is well known since the discovery of the high- $T_c$  superconductors, it is always tempting to construct a universal theory of HTSC which can naturally explain the complicated problems, such as pairing mechanism, pairing symmetry, charge stripes, etc. Because of the complexity, the dream of having such a theory is still a dream. We see that, without Hamiltonian, without wave function, without quantum field theory, our scenario has provided a beautiful and consistent picture for describing the myriad baffling microphenomena which had previously defied explanation. It would be very significant

to recall Anderson’s heuristic remark: “Many theories about electron pairing in cuprate superconductors may be on the wrong track”<sup>12</sup>. The encouraging agreement of our results with the experiments implies a possibility that our theory would finally open a new window in physics. The new ideas presented in this paper may change the way we view our world.

Finally, are there experiments left to test the conclusions of this paper? Of course, the answer is yes.

The most direct and convincing test of the theory would be the observation of the charge orders in the LSCO materials by STM. As shown in Fig. 16, our mechanism has definitively determined five abnormal phases (at  $x = 1/4$ ,  $1/8$ ,  $1/9$ ,  $1/16$  and  $1/18$ ), where the nondispersive checkerboard-type orders can coexist with the LTT original lattice ( $a = b$ ) phases of the LSCO. As we have mentioned in Sec. V that some of the relevant results have already been reported at doping levels  $x = 1/4 = 0.25$ <sup>99</sup>,  $1/8 = 0.125$ <sup>10</sup>, and  $1/16 = 0.0625$ <sup>39</sup>. It is useful to note that all the three doping parameters are a finite decimal and hence the corresponding doped samples can be easier to be obtained with high accuracy, this may explain why the charge periodic superstructures are easy to be experimentally observed close to these filling. While the other two magic doping parameters  $x = 1/9 (= 0.111 \dots)$  and  $x = 1/18 (= 0.0555 \dots)$  are a recurring decimal, as a result, the estimated nondispersive checkerboard-type ordering with periodicity  $3a \times 3a$  and  $6a \times 6a$  can only be observed in the LSCO near the doping levels  $x = 1/9$  and  $1/18$ , respectively, with much higher accuracy compared to the finite decimal doping samples.

The neutron scattering experiment can also be used to test the theory. Note that although the nondispersive  $4a \times 4a$  superstructure seems to be exactly the same in both samples ( $x = 1/8$  and  $1/16$ )<sup>10,39</sup>. We show, for the first time, that two samples are in fact very different: in the sample of  $x = 1/8$  indicated by  $p(4, 4, 1)$  in this paper, where all CuO<sub>2</sub> planes are doped; while at  $x = 1/16$  of  $p(4, 4, 2)$ , only half of the CuO<sub>2</sub> planes (every two planes) are doped. Neutron scattering would be a way to find the important difference between the “full doping” phase ( $x = 1/8$ ) and the “half doping” phase ( $x = 1/16$ ).

## Acknowledgments

The author would like to thank Ron Bourgoïn for many useful discussions and inspirational remarks.

\* Electronic address: xqhuang@nju.edu.cn

<sup>1</sup> J. G. Bednorz and K. A. Müller, Z. Phys. B **64**, 189 (1986).

<sup>2</sup> P. W. Anderson, Science **237**, 1196 (1987).

<sup>3</sup> F. C. Zhang and T. M. Rice, Phys. Rev. B **37**, 3759 (1988).

<sup>4</sup> X. G. Wen and P. A. Lee, Phys. Rev. Lett. **76**, 503 (1996).

<sup>5</sup> C. M. Varma, P.B. Littlewood, S. Schmitt-Rink, E. Abra-

- hams, and A. E. Ruckenstein, Phys. Rev. Lett. **63**, 1996 (1989); C. M. Varma, Phys. Rev. B **55**, 14554 (1997).
- <sup>6</sup> S. C. Zhang, Science **275**, 1089 (1997); H. D. Chen, S. Capponi, F. Alet, and S. C. Zhang, Phys. Rev. B **70**, 024516 (2004).
  - <sup>7</sup> E. Dagotto, Rev. Mod. Phys. **66**, 763 (1994).
  - <sup>8</sup> P. A. Lee, N. Nagaosa and X. G. Wen, Rev. Mod. Phys. **78**, 17 (2006).
  - <sup>9</sup> J. Bardeen, L. N. Cooper, and J. R. Schrieffer, Phys. Rev. **108**, 1175 (1957).
  - <sup>10</sup> T. Hanaguri *et al.*, Nature **430**, 1001 (2004).
  - <sup>11</sup> M. D. Stewart Jr., Aijun Yin, J. M. Xu, James M. Valles Jr., Science **318**, 1273 (2007).
  - <sup>12</sup> P. W. Anderson, Science **317**, 1705 (2007).
  - <sup>13</sup> Z. X. Shen *et al.*, Phys. Rev. Lett. **70**, 1553 (1993).
  - <sup>14</sup> C. C. Tsuei, J. R. Kirtley, C. C. Chi, LockSee Yu-Jahnes, A. Gupta, T. Shaw, J. Z. Sun, and M. B. Ketchen, Phys. Rev. Lett. **73**, 593 (1994).
  - <sup>15</sup> D. A. Wollman, D. J. Van Harlingen, J. Giapintzakis, and D. M. Ginsberg, Phys. Rev. Lett. **74**, 797 (1995).
  - <sup>16</sup> D. H. Wu, J. Mao, S. N. Mao, J. L. Peng, X. X. Xi, T. Venkatesan, R. L. Greene, and S. M. Anlage, Phys. Rev. Lett. **70**, 85 (1993).
  - <sup>17</sup> L. Alff, S. Meyer, S. Kleefisch, U. Schoop, A. Marx, H. Sato, M. Naito, and R. Gross, Phys. Rev. Lett. **83**, 2644 (1999).
  - <sup>18</sup> N. P. Armitage, D. H. Lu, D. L. Feng, C. Kim, A. Damascelli, K. M. Shen, F. Ronning, Z. X. Shen, Y. Onose, Y. Taguchi, and Y. Tokura, Phys. Rev. Lett. **86**, 1126 (2001).
  - <sup>19</sup> C. C. Tsuei and J. R. Kirtley, Phys. Rev. Lett. **85**, 182 (2000).
  - <sup>20</sup> A. Snezhko, R. Prozorov, D. D. Lawrie, R. W. Giannetta, J. Gauthier, J. Renaud, and P. Fournier, Phys. Rev. Lett. **92**, 157005 (2004).
  - <sup>21</sup> Ariando, D. Darminto, H. J. H. Smilde, V. Leca, D. H. A. Blank, H. Rogalla, and H. Hilgenkamp, Phys. Rev. Lett. **94**, 167001 (2005).
  - <sup>22</sup> H. Matsui, K. Terashima, T. Sato, T. Takahashi, M. Fujita, and K. Yamada, Phys. Rev. Lett. **95**, 017003 (2005).
  - <sup>23</sup> J. A. Skinta, M. S. Kim, T. R. Lemberger, T. Greibe, and M. Naito, Phys. Rev. Lett. **88**, 207005 (2002).
  - <sup>24</sup> A. Biswas, P. Fournier, M. M. Qazilbash, V. N. Smolyaninova, Hamza Balci, and R. L. Greene, Phys. Rev. Lett. **88**, 207004 (2002).
  - <sup>25</sup> A. G. Loeser, Z. X. Shen, D. S. Dessau, D. S. Marshall, C. H. Park, P. Fournier, and A. Kapitulnik, Science **273**, 325 (1996).
  - <sup>26</sup> H. Ding *et al.*, Nature **382**, 51 (1996).
  - <sup>27</sup> V. J. Emery and S. A. Kivelson, Nature **374**, 434 (1995).
  - <sup>28</sup> S. A. Kivelson, I. P. Bindloss, E. Fradkin, V. Oganessian, J. M. Tranquada, A. Kapitulnik, and C. Howald, Rev. Mod. Phys. **75**, 1201 (2003).
  - <sup>29</sup> J. M. Tranquada, B. J. Sternlieb, J. D. Axe, Y. Nakamura, and S. Uchida, Nature **375**, 561 (1995); J. M. Tranquada, J. D. Axe, N. Ichikawa, A. R. Moodenbaugh, Y. Nakamura, and S. Uchida, Phys. Rev. Lett. **78**, 338 (1997).
  - <sup>30</sup> M. R. Norman *et al.*, Nature **392**, 157 (1998).
  - <sup>31</sup> N. Ichikawa, S. Uchida, J. M. Tranquada, T. Niemöller, P. M. Gehring, S.-H. Lee, and J. R. Schneider, Phys. Rev. Lett. **85**, 1738 (2000); M. Ichikawa, E. Kaneshita, and K. Machida, J. Phys. Soc. Jpn. **70**, 33 (2001).
  - <sup>32</sup> C. Buhler, S. Yunoki, and A. Moreo, Phys. Rev. Lett. **84**, 2690 (2000).
  - <sup>33</sup> T. Hotta and E. Dagotto, Phys. Rev. Lett. **92**, 227201 (2004).
  - <sup>34</sup> K. McElroy, D. H. Lee, J. E. Hoffman, K. M. Lang, J. Lee, E. W. Hudson, H. Eisaki, S. Uchida, and J. C. Davis, Phys. Rev. Lett. **94**, 197005 (2005).
  - <sup>35</sup> J. E. Hoffman, E. W. Hudson, K. M. Lang, V. Madhavan, H. Eisaki, S. Uchida, and J. C. Davis, Science **295**, 466 (2002).
  - <sup>36</sup> C. Howald, H. Eisaki, N. Kaneko, M. Greven, and A. Kapitulnik, Phys. Rev. B **67**, 014533 (2003).
  - <sup>37</sup> T. Valla, A. V. Fedorov, J. Lee, J. C. Davis, and G. D. Gu, Science **314**, 1914 (2006).
  - <sup>38</sup> S. Komiya, H. D. Chen, S. C. Zhang, and Y. Ando, Phys. Rev. Lett. **94**, 207004 (2005); S. Komiya and Y. Ando, Phys. Rev. B **70**, 060503(R) (2004).
  - <sup>39</sup> Y. H. Kim and P. H. Hor, Mod. Phys. Lett. B **15**, 497 (2001).
  - <sup>40</sup> X. J. Zhou *et al.*, Nature **423**, 398 (2003).
  - <sup>41</sup> F. Zhou *et al.*, Physica C **408**, 430 (2004).
  - <sup>42</sup> C. Castellani, C. D. Castro, M. Grilli, and R. Perali, Physica C **341-348**, 1739 (2000).
  - <sup>43</sup> M. Franz, Science **305**, 1410 (2004).
  - <sup>44</sup> J. M. Harris, Y. F. Yan, O. K. C. Tsui, Y. Matsuda, and N. P. Ong, Phys. Rev. Lett. **73**, 1711 (1994).
  - <sup>45</sup> S. J. Hagen, C. J. Lobb, R. L. Greene, M. G. Forrester, and J. H. Kang, Phys. Rev. B **41**, 11630 (1990).
  - <sup>46</sup> T. Noda, H. Eisaki, and S. Uchida, Science **286**, 268 (1999).
  - <sup>47</sup> I. Puica, W. Lang, W. Göb, Roman Sobolewski, Phys. Rev. B **69**, 104513 (2004).
  - <sup>48</sup> K. Nakao, K. Hayashi, T. Utagawa, Y. Enomoto, and N. Koshizuka, Phys. Rev. B **57**, 8662 (1998).
  - <sup>49</sup> E. Altman and A. Auerbach, Phys. Rev. B **65**, 104508 (2002).
  - <sup>50</sup> J. E. Hirsch, Phys. Rev. B **71**, 104522 (2005).
  - <sup>51</sup> D. J. Van Harlingen, Rev. Mod. Phys. **67**, 515 (1995).
  - <sup>52</sup> S. R. White and D. J. Scalapino, Phys. Rev. B **55**, 6504 (1997).
  - <sup>53</sup> Y. Tokura, H. Takagi, and S. Uchida, Nature **337**, 345 (1989).
  - <sup>54</sup> C. C. Tsuei, and J. R. Kirtley, Rev. Mod. Phys. **72**, 969 (2000).
  - <sup>55</sup> M. M. Qazilbash, A. Biswas, Y. Dagan, R. A. Ott, and R. L. Greene, Phys. Rev. B **68**, 024502 (2003).
  - <sup>56</sup> K. A. Kouznetsov *et al.*, Phys. Rev. Lett. **79**, 3050 (1997).
  - <sup>57</sup> Qiang Li, Y. N. Tsay, M. Suenaga, R. A. Klemm, G. D. Gu, and N. Koshizuka, Phys. Rev. Lett. **83**, 4160 (1999).
  - <sup>58</sup> N. P. Armitage *et al.*, Phys. Rev. Lett. **88**, 257001 (2002).
  - <sup>59</sup> D. N. Basov and T. Timusk, Rev. Mod. Phys. **77**, 721 (2005).
  - <sup>60</sup> Guy Deutscher, Rev. Mod. Phys. **77**, 109 (2005).
  - <sup>61</sup> Ch. Renner, B. Revaz, J.-Y. Genoud, K. Kadowaki, and O. Fischer, Phys. Rev. Lett. **80**, 149 (1998).
  - <sup>62</sup> A. G. Loeser, Z.-X. Shen, M. C. Schabel, C. Kim, M. Zhang, A. Kapitulnik, and P. Fournier, Phys. Rev. B **56**, 14185 (1997).
  - <sup>63</sup> H. Ding, T. Tokoya, J. C. Campuzono, T. Takahashi, M. Randeria, M. R. Norman, T. Mochiku, K. Kadowaki and J. Giapintzakis, Nature **382**, 51 (1996).
  - <sup>64</sup> D. S. Marshall, *et al.*, Phys. Rev. Lett. **76**, 4841 (1996).
  - <sup>65</sup> X. J. Zhou *et al.*, Science **286**, 268 (1999).
  - <sup>66</sup> H. A. Mook, P. Dai, F. Dogan, and R. D. Hunt, Nature **404**, 729 (2000).
  - <sup>67</sup> M. Vershinin, S. Misra, S. Ono, Y. Abe, Y. Ando, and A.

- Yazdani, *Science* **303**, 1995 (2004).
- <sup>68</sup> S. Wakimoto, *et al.*, *Phys. Rev. B* **61**, 3699 (2000).
- <sup>69</sup> B. Keimer *et al.*, *Phys. Rev. B* **46**, 14034 (1992).
- <sup>70</sup> M. A. Kastner, R. J. Birgeneau, G. Shirane, and Y. Endoh, *Rev. Mod. Phys.* **70**, 897 (1998).
- <sup>71</sup> N. Momono, A. Hashimoto, Y. Kobatake, M. Oda, and M. Ido, *J. Phys. Soc. Jpn.* **74**, 2400 (2005).
- <sup>72</sup> M. Seul, *Science* **267**, 476 (1995).
- <sup>73</sup> N. B. Christensen, *et al.*, *Phys. Rev. Lett.* **93**, 147002 (2004).
- <sup>74</sup> S. M. Hayden, *et al.*, *Nature* **429**, 531 (2004).
- <sup>75</sup> M. K. Wu, J. R. Ashburn, C. J. Torng, P. H. Hor, R. L. Meng, L. Gao, Z. J. Huang, Y. Q. Wang, and C. W. Chu, *Phys. Rev. Lett.* **58**, 908 (1987).
- <sup>76</sup> P. Dai, H. A. Mook, and F. Dogan, *Phys. Rev. Lett.* **80**, 1738 (1998); P. Dai, H. A. Mook, S. M. Hayden, G. Aeppli, T. G. Perring, R. D. Hunt, and F. Doğan, *Science* **284**, 1344 (1999).
- <sup>77</sup> B. J. Sternlieb, J. M. Tranquada, G. Shirane, M. Sato, and S. Shamoto, *Phys. Rev. B* **50**, 12915 (1994).
- <sup>78</sup> M. Arai, T. Nishijima, Y. Endoh, T. Egami, S. Tajima, K. Tomimoto, Y. Shiohara, M. Takahashi, A. Garrett, and S. M. Bennington, *Phys. Rev. Lett.* **83**, 608 (1999).
- <sup>79</sup> B. Fauqué, Y. Sidis, V. Hinkov, S. Pailhès, C. T. Lin, X. Chaud, and P. Bourges, *Phys. Rev. Lett.* **96**, 197001 (2006).
- <sup>80</sup> S. D. Wilson, P. C. Dai, S. L. Li, S. X. Chi, H. J. Kang, J. W. Lynn, *Nature* **442**, 59 (2006).
- <sup>81</sup> J. -P. Ismer, Ilya Eremin, Enrico Rossi, and Dirk K. Morr, *Phys. Rev. Lett.* **99**, 047005 (2007).
- <sup>82</sup> V. L. Ginzburg and L. D. Landau, *Zh. Eksp. Teor. Fiz.* **20**, 1064 (1950).
- <sup>83</sup> M. Uchida, Y. Onose, Y. Matsui, and Y. Tokura, *Science* **311**, 359 (2006).
- <sup>84</sup> S. Sugai, Y. Takayanagi, and N. Hayamizu, *Phys. Rev. Lett.* **96**, 137003 (2006).
- <sup>85</sup> A. R. Moodenbaugh, Y. Xu, M. Suenaga, T. J. Folkerts and R. N. Shelton, *Phys. Rev. B* **38**, 4596 (1988).
- <sup>86</sup> M. K. Crawford, R. L. Harlow, E. M. McCarron, W. E. Farneth, J. D. Axe, H. Chou, and Q. Huang, *Phys. Rev. B* **44**, 7749 (1991).
- <sup>87</sup> C. C. Homes, S. V. Dordevic, G. D. Gu, Q. Li, T. Valla, and J. M. Tranquada, *Phys. Rev. Lett.* **96**, 257002 (2006).
- <sup>88</sup> M. Fujita, H. Goka, K. Yamada, J. M. Tranquada, and L. P. Regnault, *Phys. Rev. B* **70**, 104517 (2004).
- <sup>89</sup> A. Melikyan and Z. Tešanović, *Phys. Rev. B* **71**, 214511 (2005).
- <sup>90</sup> P. Wróbel, *Phys. Rev. B* **74**, 014507 (2006).
- <sup>91</sup> P. Dai, H. A. Mook, R. D. Hunt, and F. Doğan, *Phys. Rev. B* **63**, 054525 (2001).
- <sup>92</sup> V. F. Mitrovic, E. E. Sigmund, M. Eschrig, H. N. Bachman, W. P. Halperin, A. P. Reyes, P. Kuhns, and W. G. Moulton, *Nature* **413**, 501 (2001).
- <sup>93</sup> H. D. Chen, O. Vafek, A. Yazdani, and S. C. Zhang, *Phys. Rev. Lett.* **93**, 187002 (2004).
- <sup>94</sup> H. Y. Chen and C. S. Ting, *Phys. Rev. B* **71**, 220510(R) (2005).
- <sup>95</sup> S. Sachdev, *Science* **288**, 475 (2000).
- <sup>96</sup> D. Podolsky, E. Demler, K. Damle, and B. I. Halperin, *Phys. Rev. B* **67**, 094514 (2003).
- <sup>97</sup> Z. Tešanović, *Phys. Rev. Lett.* **93**, 217004 (2004).
- <sup>98</sup> J. B. Goodenough, J. -S. Zhou, and J. Chan *Phys. Rev. B* **47**, 5275 (1993); J. B. Goodenough, *Europhys. Lett.* **57**, 550 (2002).
- <sup>99</sup> S. Wakimoto, K. Yamada, J. M. Tranquada, C. D. Frost, R. J. Birgeneau, and H. Zhang, *Phys. Rev. Lett.* **98**, 247003 (2007).
- <sup>100</sup> A. Ino, C. Kim, M. Nakamura, T. Yoshida, T. Mizokawa, Z. -X. Shen, A. Fujimori, T. Kakeshita, H. Eisaki, and S. Uchida, *Phys. Rev. B* **62**, 4137 (2000).
- <sup>101</sup> Øystein Fischer, Martin Kugler, Ivan Maggio-Aprile, Christophe Berthod, and Christoph Renner, *Rev. Mod. Phys.* **79**, 353 (2007).
- <sup>102</sup> J. Nagamatsu *et al.*, *Nature* **410**, 63 (2001).
- <sup>103</sup> J. M. Williams *et al.*, *Science* **252**, 1501 (1991).